

# Active Control to Improve the Aerodynamic Performance and Reduce the Tip Clearance Noise of Axial Turbomachines

Lars Neuhaus\* and Wolfgang Neise†

German Aerospace Center, Institute of Propulsion Technology, Turbulence Research Department, 10623 Berlin, Germany

The tip clearance flow of axial turbomachines is important for their aerodynamic and acoustic performance. The rotating instability phenomena and the tip clearance noise are observed on axial turbomachines with larger tip clearances. In this paper it is shown that it is possible to reduce the tip clearance noise and improve the aerodynamic performance of the fan by actively controlling the tip clearance flow. To achieve this, air is injected into the gap either through slits in the casing wall or through the rotor blades and out of the blade tips.

The experiments were made with a high-pressure axial fan of  $D = 452.4$  mm impeller diameter connected to an anechoically terminated outlet duct. The fan has 24 rotor blades and 17 stator vanes. Two tip clearance gaps  $\zeta = 0.7\%$  and  $5.6\%$  of the blade chord length are used.

Three configurations for air injection through the casing wall are investigated: 24 and 17 slit nozzles, and a uniform circumferential slit. With steady air injection through the optimum configuration it is possible to achieve significant improvements of the aerodynamic performance and of the radiated noise level.

Air injection out of the tip of the impeller blades is also effective in improving the aerodynamic and acoustic performance of the fan.

The rotating instability components and the tip clearance noise can be suppressed with both injection methods.

In case of the smaller tip clearance gap, the range of stable fan operation is enlarged.

## Nomenclature

$A$	cross sectional area ( $A_0 = 1 \text{ m}^2$ )	$Q$	volume flow ( $Q_0 = 1 \text{ m}^3/\text{s}$ )
$a_0$	speed of sound	$s$	tip clearance
$a_\theta$	azimuthal phase angle velocity	$u$	flow velocity
$b$	variable	$u_{in}$	jet exit flow velocity
$c$	blade chord length	$U$	impeller tip speed
$D$	impeller diameter	$V$	number of stator vanes
$f$	frequency	$Z$	number of impeller blades
$f_{LRD}$	rotating frequency of the impeller	$Z_{noz}$	number of injection nozzles
$h$	harmonic order of the blade passing frequency		
$L_p$	pressure level	$\varepsilon$	hub-to-tip ratio
$L_W$	sound power level	$\zeta$	$= s/c$ ; non-dimensional tip clearance
$m$	azimuthal mode order	$\eta_{el}$	efficiency of the drive motor
$m_{in}$	injected mass flow in percent of the mass flow delivered by the fan at $\varphi = 0.3$	$\eta_t$	$= \Delta p_t / (Q / (\eta_{el} P_{el} + P_{in}))$ approximate total fan efficiency
$M$	$= u/a_0$ ; flow Mach number	$\theta$	blade stagger angle
$M_{Tip}$	Mach number at the impeller blade tip	$\Omega$	$= 2\pi f_{LRD}$ ; angular velocity
$n$	impeller speed	$\omega_\theta$	phase angle velocity
$\Delta p_t$	total fan pressure ( $\Delta p_{t0} = 1 \text{ Pa}$ )	$\rho_0$	air density
$P_{el}$	electric power input to drive motor	$\varphi$	$= 4Q / (\pi D^2 U)$ ; flow coefficient
$P_{in}$	$= M_{in} u_{in}^2$ aerodynamic power of injected air flow	$\psi$	$= 2\Delta p_t / (\rho_0 U^2)$ ; pressure coefficient

\* Dipl.-Ing., DLR, Müller-Breslau-Str. 8, 10623 Berlin, Germany.

† Prof. Dr.-Ing., DLR, Müller-Breslau-Str. 8, 10623 Berlin, Germany.

## I. Introduction

Axial turbomachines have a radial gap between the casing and the rotor blades. The static pressure difference between the suction and the pressure side of the impeller blades produces a secondary flow over the tip of the rotor blades (Figure 1a). This tip clearance flow is important for the aerodynamic and acoustic performance of the machine. Pressure rise and efficiency drop, and the usable range of the performance characteristics is diminished as the rotor flow is stalled at higher flow rates.

Previous work at DLR-Berlin<sup>1-4</sup> investigating the effects of varying tip clearances on noise and performance showed the existence of a broad-band noise source for large clearances. This source appeared in the rotor wall pressure spectrum at about half the blade passing frequency (BPF) and radiated a fluctuating tonal component into the far field, the tip clearance noise (TCN). Interpretation of the spectra and circumferential mode analyses led to the model of a rotating source mechanism, called rotating instability (RI), which moves relative to the blade row at a fraction of the shaft speed, similar to the cells of rotating stall (Kameier<sup>1</sup>, Kameier and Neise<sup>2</sup>). The effect was also observed in the third stage of the low-speed research compressor at the TU Dresden when the tip clearance was enlarged (Mailach et al.<sup>5</sup>). Legros et al.<sup>6</sup> have found rotating instability as noise source of the axial fan in air condition systems for commercial aircrafts.

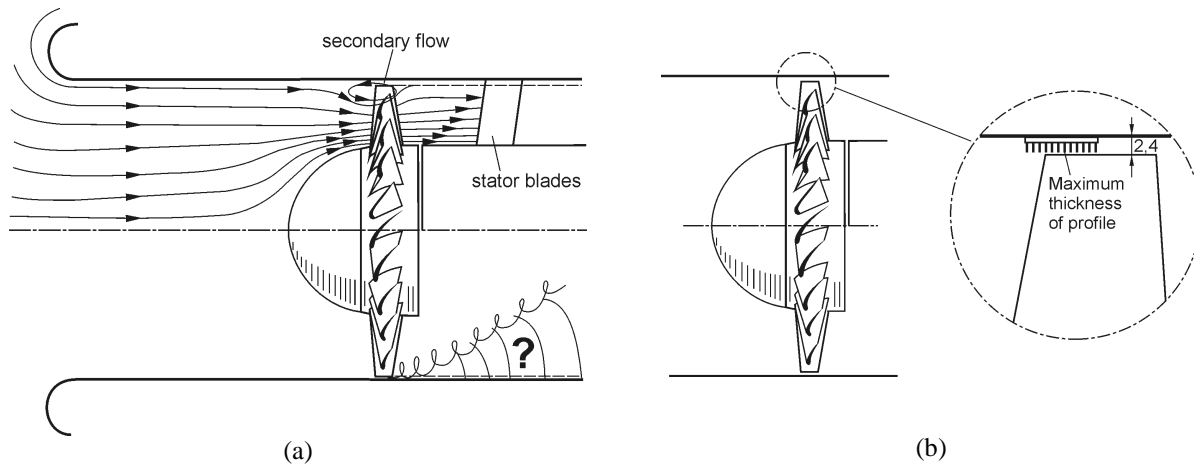


**Figure 1: Schematic view of (a) the secondary flow through the tip clearance gap and (b) of a turbulence generator inserted in the gap.**

Kameier<sup>1</sup> was successful in reducing the tip clearance noise and increasing the aerodynamic performance by mounting a turbulence generator into the tip clearance gap (Kameier<sup>1</sup>, Kameier and Neise<sup>3</sup>), compare Figure 1b. The aim of the present work is to reproduce and possibly improve the effect achieved with the turbulence generator without modifications of the tip clearance gap itself to make the method applicable also to flow machines where the tip clearance gap is variable, e.g., due to usage of different stagger angles of the impeller blades.

One method for increasing aerodynamic performance and reducing radiated noise level is to control the flow in tip clearance gap with air injection into the gap. A number of authors reported successful application of air injection upstream of the fan rotor to inhibit rotating stall and compressor surge (D'Andrea et al.<sup>7</sup>, Weigl et al.<sup>8</sup>, Spakovszky et al.<sup>9, 10</sup>) or to increase the usable range of the performance characteristic (Nie et al.<sup>11</sup>). Efficiency and noise emission were not addressed in the studies mentioned above. Neuhaus and Neise<sup>12, 13</sup> investigated the influence of air injection on pressure rise, efficiency, increased stall margin, and noise emission.

## II. Experimental Facility

The test fan is a low-speed high-pressure axial fan with outlet guide vanes, the same as used for the experiments in references 1 - 4. The principal impeller dimensions are as follows: impeller diameter  $D = 452.4$  mm; hub-to-tip ratio  $\varepsilon = 0.62$ ; NACA 65 blade profile; blade number  $Z = 24$ ; blade chord length at the tip  $c = 43$  mm; maximum blade thickness 3 mm; blade stagger angle at the tip  $\theta = 27^\circ$ . The design speed is  $n = 3000$ /min. The stator row comprises  $V = 17$  unprofiled vanes. The axial distance between rotor and stator at the outer circumference is  $\Delta x/c = 1.3$ . The tip clearance can be varied by exchanging casing segments while the impeller diameter remains constant. Four casing segments are available to give the following tip clearances:  $s = 0.3, 0.6, 1.2,$  and  $2.4$  mm ( $\zeta = s/c = 0.7\%, 1.4\%, 2.8\%,$  and  $5.6\%$ ).

Figure 2 shows the experimental setup with its major dimensions. The measurement facility is in accordance with the requirements of DIN 24136<sup>14</sup> for measurement of aerodynamic fan performance. On the inlet side there is a short duct section with a bellmouth nozzle; there are no flow straighteners or screens in the inlet duct. The anechoically terminated outlet duct is in accordance with the international standard ISO 5136<sup>15</sup>.

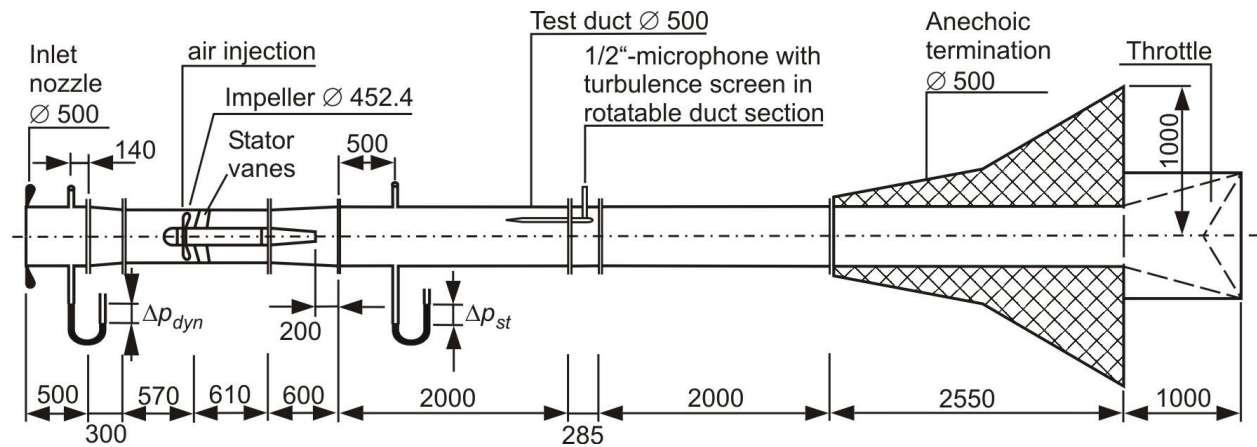


**Figure 2: Schematic view of the experimental setup (dimensions in mm).**

In the outlet duct a 1/2-inch microphone equipped with a turbulence screen is mounted in a rotatable duct section to measure the circumferentially averaged sound pressure level at a specified radial distance from the duct axis. To measure the unsteady blade pressures for the experiments described in chapters III and V, a miniature pressure sensor is mounted on the suction side of one impeller blade at 36% of the chord length without changing the original outer blade contour. The radial distance from the blade tip is 7% of the chord length. To measure the unsteady casing wall pressures discussed in chapter IV, a conventional static pressure tap is used to which a 1/4-inch microphone is connected via a suitable coupling device. The acoustic frequency response of the pressure tap / coupler combination is flat in magnitude and phase within the frequency range interested here, i.e. 0 – 1.6 kHz. The axial position of the 1/4-inch microphone is 0.3 mm upstream the impeller blades.

To control the flow conditions in the tip clearance gap, air is injected into the gap through different injection configurations. In the first, 24 slit nozzles mounted flush with the inner casing wall are distributed uniformly over the circumference of the casing. In the second configuration 17 nozzles are employed instead of 24; otherwise the arrangement is the same as before. In the third injection configuration the individual nozzles are replaced by a continuous circumferential slit. The axial position of all three injection configurations is  $\xi = x/c = 16.6\%$  downstream of the leading edge of the rotor blades which is the point of the maximum profile thickness of the impeller blade, as shown in Figure 3. In earlier experiments by Neuhaus and Neise<sup>16</sup>, this axial position was found to be the optimal one for the air injection. The angle between the jet axis and the interior casing wall is 15°. Circumferentially, the jet direction is equal to the main flow direction in the fan duct.

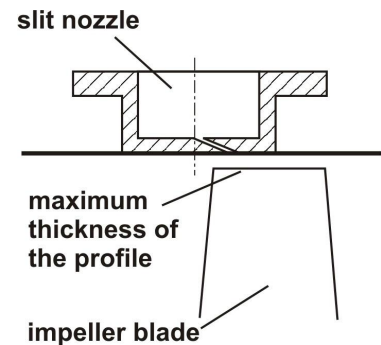


**Figure 3: Schematic view of a slit nozzle at the axial position  $\xi = 16.6\%$ .**

In the fourth injection configuration, the air is not blown through the casing wall, but through the rotor blades and exiting from the blade tips. In this particular impeller, a small tube reaching from the hub to the blade tip is inserted into each of the  $Z = 24$  blades. Compressed air is fed through the hollow shaft of the electric drive motor into a plenum chamber located in the spinner of the fan. From there the compressed air is guided through the tubes to the blade tips and blown into the tip clearance gap. The axial position of the air outlet openings in the tip is  $\xi = x/c = 16.6\%$ , the same as before in the other three injection configurations. The angle between the jet axis and the blade tip surface is 45°.

### III. Air Injection Through the Fan Casing

In this paper only results for steady air injection are presented. Results for pulsed injection are reported in references 12 and 13. As mentioned before, the axial position used here is the optimal position with regard to the needed injection rate, compare Neuhaus and Neise<sup>16</sup>.

#### A. Steady air injection through 24 slit nozzles

The first experiments were conducted with steady air injection using  $Z_{noz} = Z = 24$  nozzles which is equal to the number of impeller blades. With this arrangement it was possible to control the tip vortex of each impeller blade at the same time. Measurements were made at the design impeller speed  $n = 3000/\text{min}$ . Experiments at reduced speed are shown in the references 12 and 13.

Figure 4 shows the aerodynamic and acoustic performance curves at the design speed. For symbols and the definitions of the non-dimensional fan performance parameters used, see the nomenclature. The injected mass flow is given in percent of the maximum mass flow delivered by the fan (i.e., at  $\varphi = 0.3$ ). With steady air injection, pressure rise and efficiency increase at low flow rates, and the stall point is shifted towards lower flow rates. In case of the injection rate  $m_{in} = 0.8\%$ , the stall point is shifted to the operating point  $\varphi = 0.161$ , i.e., the useful range of the fan characteristic is enlarged by 36%; at this point the fan pressure is increased by about 28% and the efficiency by about 10%. With mass flow injection rates of  $m_{in} = 0.6\%$  and  $0.8\%$ , the optimum efficiency is increased, and for even higher injection rates (not shown here), the maximum efficiency decreases slightly.

Note that the aerodynamic power of the injected air flow is taken into account when calculating the fan efficiency, compare the equation given in the nomenclature. This is true for all efficiency data presented in this paper.

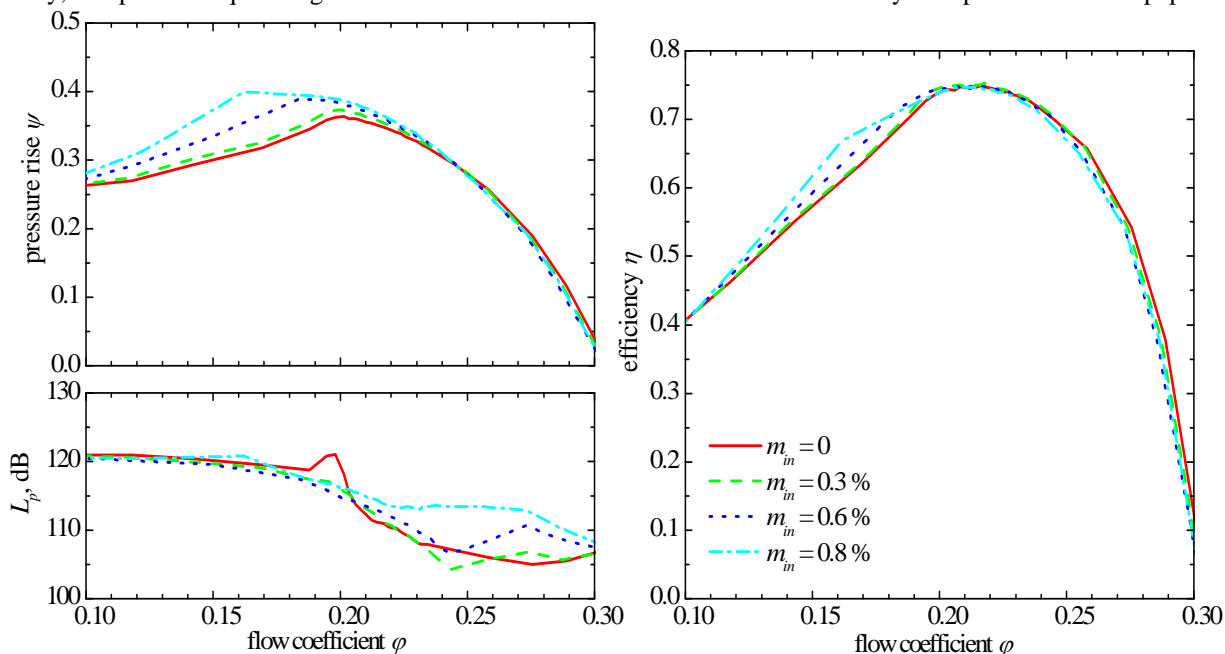


**Figure 4: Pressure coefficient, efficiency, and sound pressure level in the outlet duct as functions of the flow coefficient for different steady air injection mass flow rates;  $n = 3000/\text{min}$ ,  $Z_{noz} = 24$ ,  $\zeta = 5.6\%$ ,  $\xi = 16.6\%$ .**

The sound pressure characteristic without air injection exhibits a peak at operating points around  $\varphi = 0.2$  which is caused by tip clearance noise. With air injection, the noise level is reduced in this range. At higher flow rates, the level in the outlet duct increases with the injected mass flow. At lower flow rates, the noise is nearly the same as without air injection. When the injected air flow is increased further ( $m_{in} > 0.8\%$ , not shown here), the sound pressure level is larger than without air injection, except for the operating points where tip clearance noise exists.

The influence of the air injection on rotating instability and tip clearance noise is shown in Figure 5 where sound power spectra in the fan outlet duct and wall pressure spectra on the suction side of a rotor blade are plotted for the operating point  $\varphi = 0.2$  where tip clearance noise is strong. Without air injection and for  $m_{in} = 0.3\%$ , rotating instability is visible in the blade wall pressure spectrum and tip clearance noise in the outlet duct. When the injected mass flow rate is  $m_{in} = 0.6\%$ , both of these components disappear.

The level of the blade passing frequency (BPF) is found to increase with the injected air flow which is due to the interaction between the jets from the  $Z_{noz}$  nozzles and the  $Z$  impeller blades. The azimuthal mode order  $m$  of the BPF-component generated by this interaction can be determined following Tyler and Sofrin's<sup>11</sup> rotor-stator-interaction theory

$$m = hZ + bZ_{noz} \quad (1)$$

where  $h = 1, 2, 3, \dots$  for the BPF fundamental and harmonics, and  $b = \dots, -2, -1, 0, 1, 2, \dots$

With  $Z_{noz} = Z = 24$  nozzles in the present configuration, the interaction mode order is  $m = 0$ , i.e., the plane wave which is propagational in the outlet duct at all frequencies.

Despite the increase in BPF-level, the overall sound pressure level is reduced, e.g., from 121 dB to 113 dB at  $m_{in} = 0.6\%$  while the BPF level increases from 104 dB to 112 dB. For higher injection rates, the blade tone level rises even more which limits the usefulness of the method despite the improvement in aerodynamic performance and reduction in tip clearance noise.

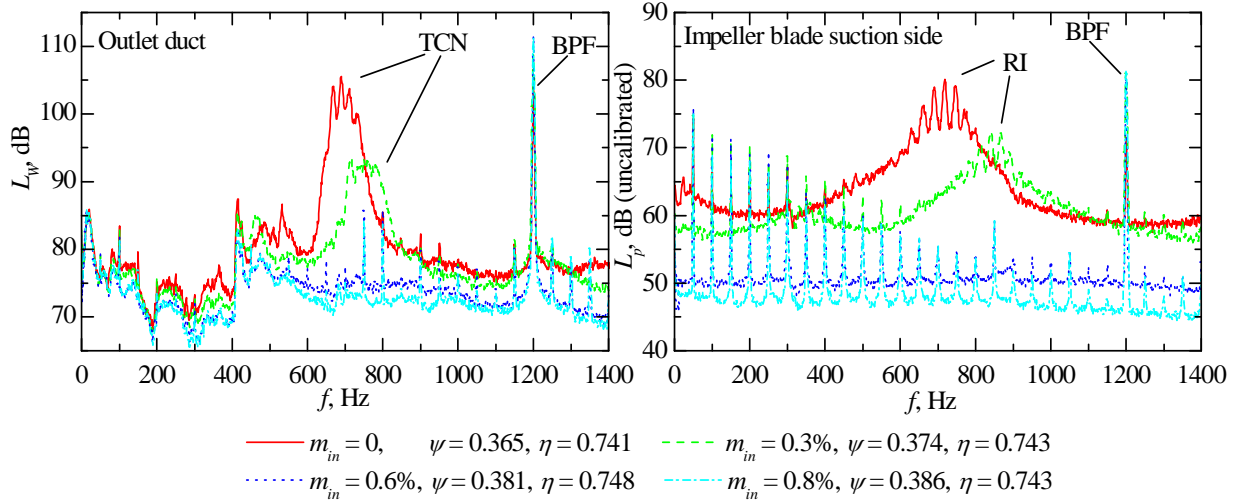


**Figure 5: Sound power spectra in the fan outlet duct and wall pressure spectra on the rotor blade suction side for different steady air injection rates;  $n = 3000/\text{min}$ ,  $Z_{noz} = 24$ ,  $\zeta = 5.6\%$ ,  $\xi = 16.6\%$ ,  $\varphi = 0.2$ .**

### B. Steady air injection through 17 slit nozzles

To avoid the increase in BFP-level, the number of nozzles is changed to obtain a cut-off rotor-jet-interaction, similar to the choice of the number of stator vanes in modern aero engine design. The angular phase velocity  $\omega_\theta$  of the rotor-jet-interaction pressure fluctuations is given by

$$\omega_\theta = \frac{hZ\Omega}{hZ + bZ_{noz}} = \frac{\Omega}{1 + \frac{bZ_{noz}}{hZ}}, \quad (2)$$

and the corresponding azimuthal phase velocity  $a_\theta$  at the casing wall is

$$a_\theta = \omega_\theta \frac{D}{2}. \quad (3)$$

The rotor tip speed Mach number is

$$M_{tip} = \frac{\Omega D}{2a_0}. \quad (4)$$

A cut-off rotor-jet-interaction mode is obtained when the azimuthal phase velocity at the casing wall becomes subsonic, i.e., when

$$\omega_\theta \frac{D}{2} < a_0 \quad (5)$$

$$\Rightarrow |hZ + bZ_{noz}| > hZ \cdot M_{Tip} \quad (6)$$

For positive values of  $b$ , the above condition is always fulfilled. For negative values, two solutions exist:

$$hZ + bZ_{noz} > hZ \cdot M_{Tip} \Rightarrow -bZ_{noz} < hZ \cdot (1 - M_{Tip}) \quad (6)$$

$$-hZ - bZ_{noz} > hZ \cdot M_{Tip} \Rightarrow -bZ_{noz} > hZ \cdot (1 - M_{Tip}) \quad (7)$$

For the present experiments, 17 injection nozzles are chosen to give a rotor-jet-interaction mode order of  $m = 7$ . This mode cannot propagate through the fan duct at the blade passing frequency, i.e., it decays exponentially with increasing axial distance from the source (interaction region).

Figure 6 shows the aerodynamic and acoustic performance curves with the air injection rate as a parameter for  $Z_{noz} = 17$  nozzles at the design speed. With air injection, the fan pressure is improved at low flow rates and the stall point is shifted towards lower flow rates. With small injection rates, the fan efficiency is improved at low mean flow rates ( $\varphi < 0.19$ ).

With the largest injection rate  $m_{in} = 1.5\%$ , the fan pressure is increased over the entire characteristic curve. The usable range of the fan characteristic is enlarged by 48%, and at the operating point  $\varphi = 0.149$  the fan pressure is raised from  $\psi = 0.29$  to 0.41. However, the fan efficiency is impaired over a large regime of the fan characteristics because of the high power which is necessary to enforce the high velocity of the air jets.

The range of operating conditions over which the sound pressure level is reduced increases with the injected mass flow. Only for the largest injection rate ( $m_{in} = 1.5\%$ ) and mean flow rates  $\varphi > 0.235$ , the radiated level is higher than without air injection. The optimum injection rate depends on the operating point: for  $\varphi < 0.185$  the maximum level reduction is obtained with  $m_{in} = 1.5\%$  and for  $\varphi > 0.185$  with  $m_{in} = 0.6\%$ .

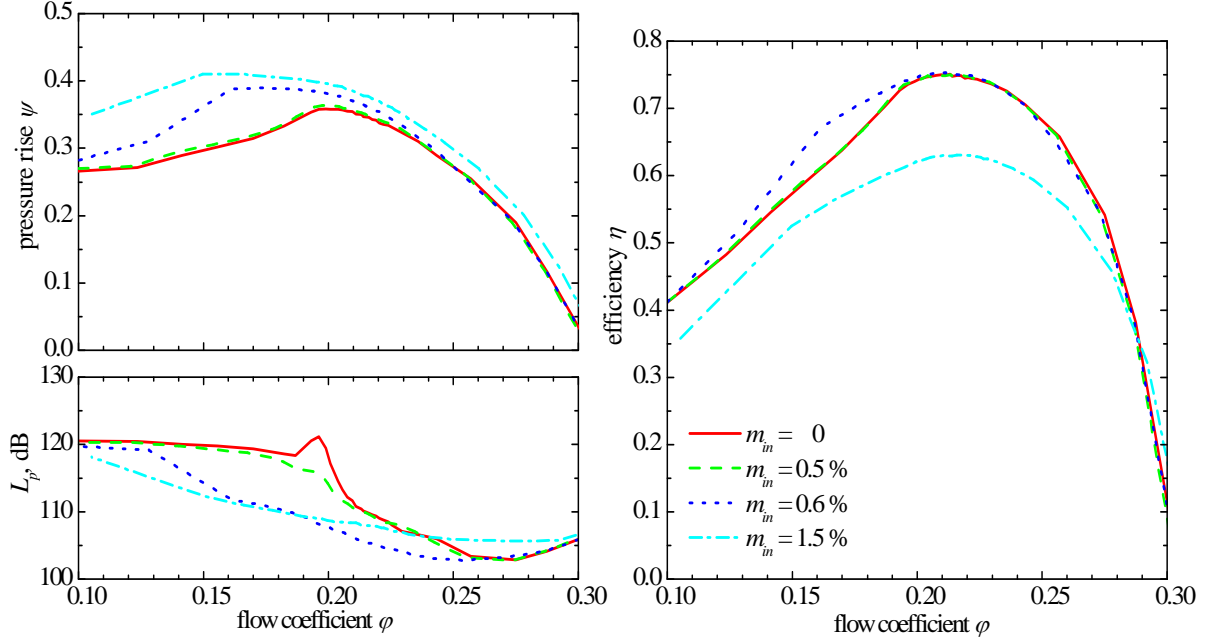


**Figure 6: Pressure coefficient, efficiency, and sound pressure level in the outlet duct as functions of the flow coefficient for different steady air injection mass flows;  $n = 3000/\text{min}$ ,  $Z_{noz} = 17$ ,  $\zeta = 5.6\%$ ,  $\xi = 16.6\%$ .**

The sound power spectra in the outlet duct and the wall pressure spectra on the suction side of one rotor blade are shown in Figure 7, again for the operating point  $\varphi = 0.2$  where tip clearance noise is strong. Rotating instability and tip clearance noise are visible in the spectra for zero injected mass flow and for  $m_{in} = 0.5\%$ . For higher mass flow rates  $m_{in} \geq 0.6\%$ , rotating instability and tip clearance noise are suppressed. The BPF-level in the outlet duct no longer increases when the injection rate goes up, but remains almost constant at about 96 dB. Incidentally, a strong peak appears at 850 Hz in the blade wall pressure spectra. This “jet-passing-frequency” is picked up by the sensor mounted on one impeller blade which crosses 17 jets during each revolution. In the fixed frame of reference, i.e., the fan outlet duct, this frequency component does not exist.

With the cut-off injection design employing 17 nozzles in the present case, the overall sound pressure level in the outlet duct can be lowered from 119 dB at the operating point  $\phi = 0.2$  down to 106 dB with  $m_{in} = 0.6\%$  and to 108 dB with  $m_{in} = 1.5\%$ .

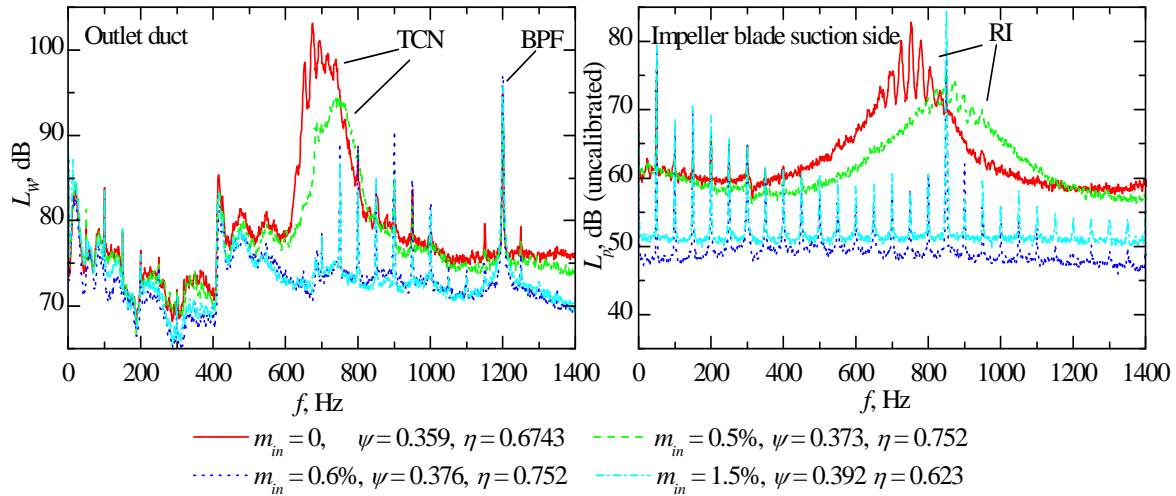


**Figure 7: Sound power spectra in the fan outlet duct and wall pressure spectra on the rotor blade suction side for different steady air injection rates;  $n = 3000/\text{min}$ ,  $Z_{noz} = 17$ ,  $\zeta = 5.6\%$ ,  $\xi = 16.6\%$ ,  $\phi = 0.2$ .**

### C. Steady air injection through a circumferential slit arrangement

Another method to avoid the increases in fan tone level due to rotor-jet-interaction is to inject air through a continuous and uniform circumferential slit, see the schematic depicted in Figure 8. With this configuration, there are no individual jets and, therefore, no noise generating interactions with the rotor blades.

The results obtained with the continuous slit injection are shown in Figure 9 and Figure 10. The usable range of the fan characteristic is enlarged monotonously with the injected mass flow. With  $m_{in} = 1.5\%$ , the improvement amounts to 62%, and at the operating point  $\phi = 0.137$ , the fan pressure increases from  $\psi = 0.29$  to 0.41

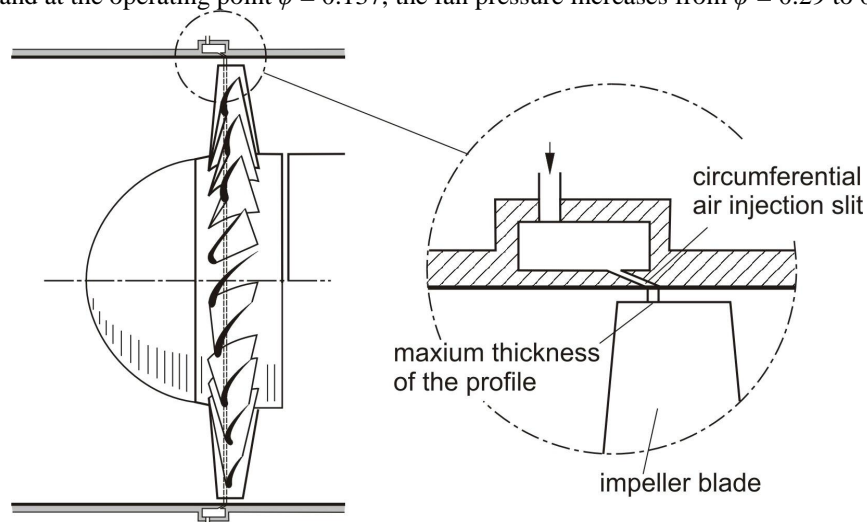


**Figure 8: Schematic view of the circumferential slit arrangement.**

The efficiency increases with air injection only at low flow rates. With the mass flow injection rates  $m_{in} = 0.5\%$  and  $0.8\%$ , the optimum efficiency is increased. With  $m_{in} = 1.5\%$ , the efficiency decreases slightly to the right of the optimum fan efficiency. Again, the optimum air injection rate depends on the operating point. A comparison of the fan efficiency data obtained with the continuous slit arrangement and with the “cut-off design” (section III B), both with  $m_{in} = 1.5\%$  mass flow rate, reveals the influence of the injection velocity on the aerodynamic power necessary to produce it: Lower jet injection velocities require a smaller amount of power than larger ones and, therefore, are better for good fan aerodynamic efficiency.

The radiated sound pressure level is reduced over a large range of flow rates. The higher the injection rate, the larger the regime of flow coefficients with reduced sound pressure level. At the operating point  $\varphi = 0.2$ , the overall sound pressure level in the outlet duct is reduced from 117 dB down to 106 dB with  $m_{in} = 0.8\%$  injection rate and to 105 dB with  $m_{in} = 1.5\%$ .

When the injected air flow is  $m_{in} = 0.5\%$ , rotating instability is still visible in the blade wall pressure spectrum and tip clearance noise in the sound power spectrum, compare Figure 10. Beginning at  $m_{in} = 0.8\%$ , rotating instability and tip clearance noise disappear. The BPF-level decreases from 95 dB to 92 dB when the air injection rate is raised up to 1.5%. Hence, with the continuous slit arrangement, the improvements in aerodynamic performance are accompanied by lower noise levels.

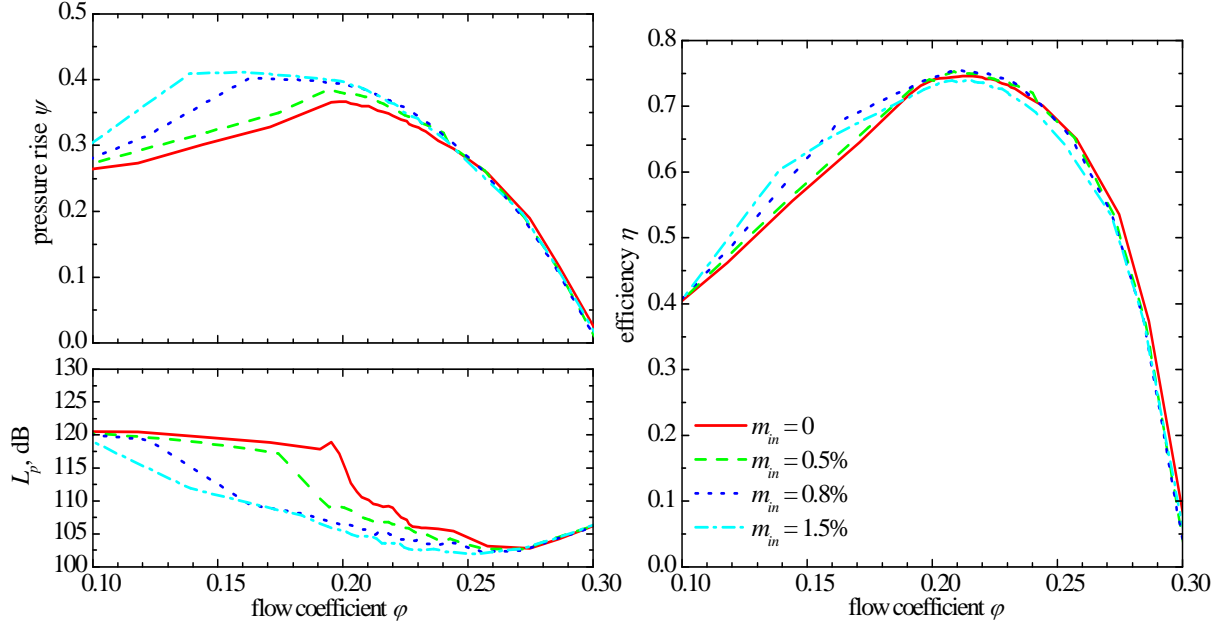


**Figure 9: Pressure coefficient, efficiency, and sound pressure level in the outlet duct as functions of the flow coefficient for different steady air injection mass flows injected through the continuous slit arrangement;  $n = 3000/\text{min}$ ,  $\zeta = 5.6\%$ ,  $\xi = 16.6\%$ .**

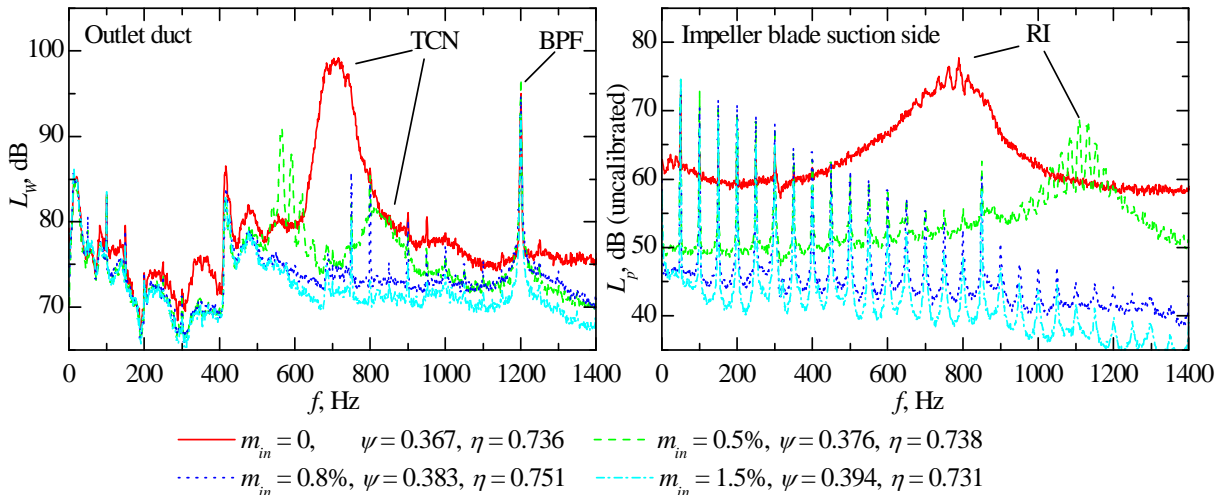


**Figure 10: Sound power spectra in the fan outlet duct and wall pressure spectra on the rotor blade suction side for different steady air injection rates through the continuous slit arrangement;  $n = 3000/\text{min}$ ,  $\zeta = 5.6\%$ ,  $\xi = 16.6\%$ ,  $\varphi = 0.2$ .**



#### IV. Steady Air Injection Out of the Rotor Blade Tips

In this method, control of the blade tip vortex flow is attempted by injecting air into the tip clearance gap through the blades and out of their tip surfaces. In these flow control experiments the test fan had to be run at a reduced speed of  $n = 1800/\text{min}$  because of a limitation in the injected mass flow that could be forced through the small diameter tubes by the available compressed air supply. The tubes connect the pressure reservoir in the fan hub with the impeller blade tips.

The results for the aerodynamic fan performance are shown in Figure 11. Fan pressure and efficiency increase over the whole range of operating conditions. The usable range of the fan characteristic is enlarged by 38%, and at the operating point  $\phi = 0.175$ , fan pressure and efficiency increase from  $\psi = 0.32$  to 0.41 and  $\eta = 0.51$  to 0.62 when the injected mass flow rate is moderate,  $m_{in} = 0.3\%$ . The sound pressure level radiated into the outlet duct is reduced significantly, depending on the operating condition.

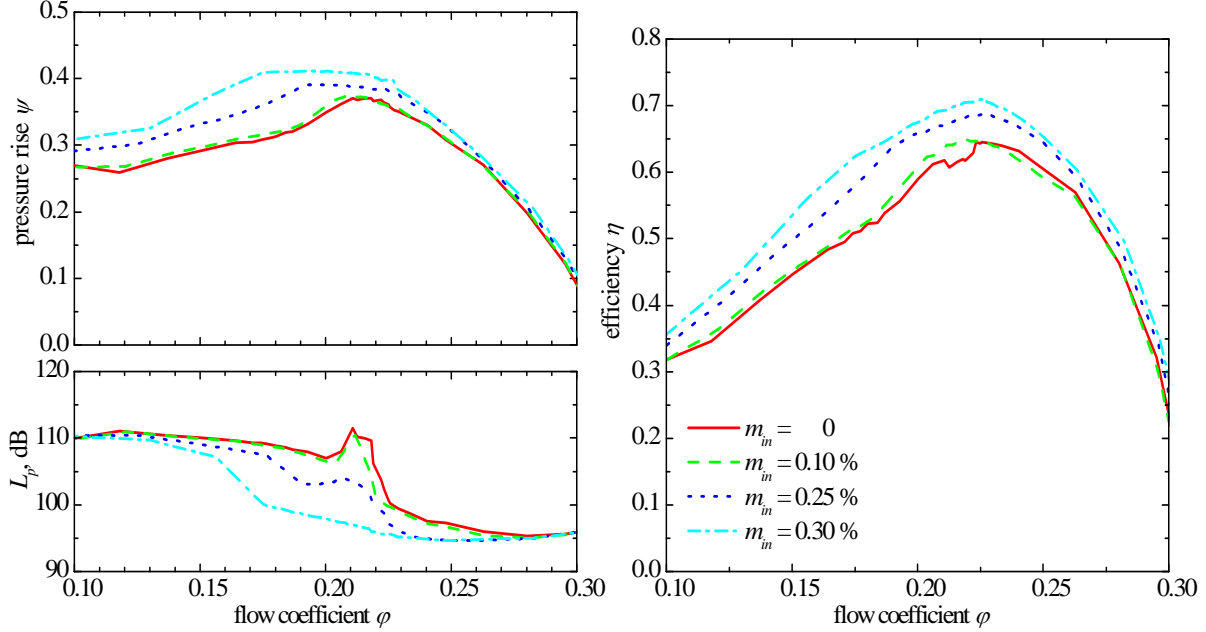


Figure 11: Pressure coefficient, efficiency, and sound pressure level in the outlet duct as functions of the flow coefficient for different steady air injection mass flows out of the impeller blade tip;  $n = 1800/\text{min}$ ,  $\zeta = 5.6\%$ ,  $\xi = 16.6\%$ .

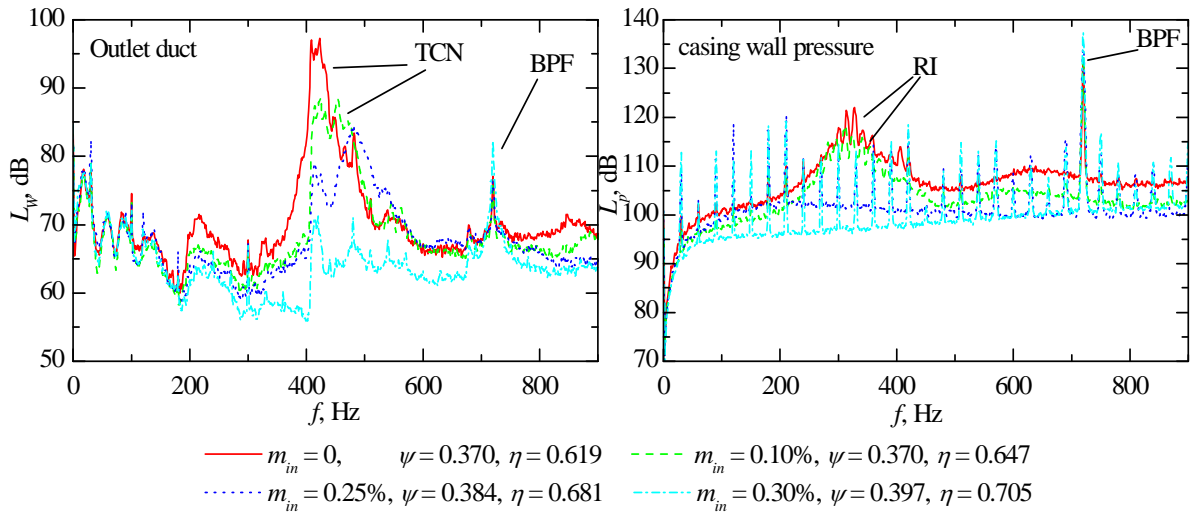


Figure 12 Sound power spectra in the fan outlet duct and wall pressure spectra on the rotor blade suction side for different steady air injection rates out of the impeller blade tip;  $n = 1800/\text{min}$ ,  $\zeta = 5.6\%$ ,  $\xi = 16.6\%$ ,  $\phi = 0.22$ .

Figure 12 shows the sound power spectra in the outlet duct and the pressure spectra measured at the interior casing wall at the operating point  $\varphi = 0.22$  where tip clearance noise and rotating instability are pronounced in the uncontrolled state. Rotating instability and tip clearance noise are clearly visible when the injected mass flow is up to  $m_{in} = 0.25\%$  and are completely suppressed when the injected mass flow is raised to  $m_{in} = 0.30\%$ . The overall sound pressure level is reduced from 109 dB to 102 dB with  $m_{in} = 0.25\%$  and to 96 dB with  $m_{in} = 0.3\%$ , however, for unknown reasons, the BPF-level increases from 77 dB without air injection to 82 dB with  $m_{in} = 0.3\%$ .

## V. Experiments with a Smaller Tip Clearance Gap

The previous discussion has shown that air injection into the tip clearance gap is appropriate to improve the aerodynamic and acoustic performance of axial-flow fans. The results that have been presented in this paper so far are for a large tip clearance gap of  $\zeta = s/c = 5.6\%$  of the blade chord at the tip.

In this chapter, the potential of the flow control method for a small tip clearance gap of  $\zeta = 0.7\%$  is examined. Only data for the aerodynamic fan performance are reported, see Figure 13. For these experiments, the continuous slit arrangement in the fan casing was used for air injection into the tip clearance gap. For comparison, the results for the large tip clearance gap ( $\zeta = 5.6\%$ ) are depicted in Figure 9.

The stall point of the fan without air injection is  $\varphi = 0.2$  for the large and  $\varphi = 0.153$  for the small tip clearance gap. For both the small and the large tip clearance gap, the usable range of the performance curve is enlarged quite substantially, e.g., from 0,153 to 0,115 with  $m_{in} = 1.5\%$  in case of the small tip clearance. However, while there is a positive effect of the air injection over a wide range of operating conditions when the tip clearance is large, a beneficial effect can be observed for the small tip clearance gap only at operating conditions where the blade flow with no control attempt is stalled. At these operating points, fan pressure and efficiency increase, and the radiated noise is reduced with increasing injected mass flow. At operating points with stable flow conditions, no effect or a negative one is observed as a result of the air injection.

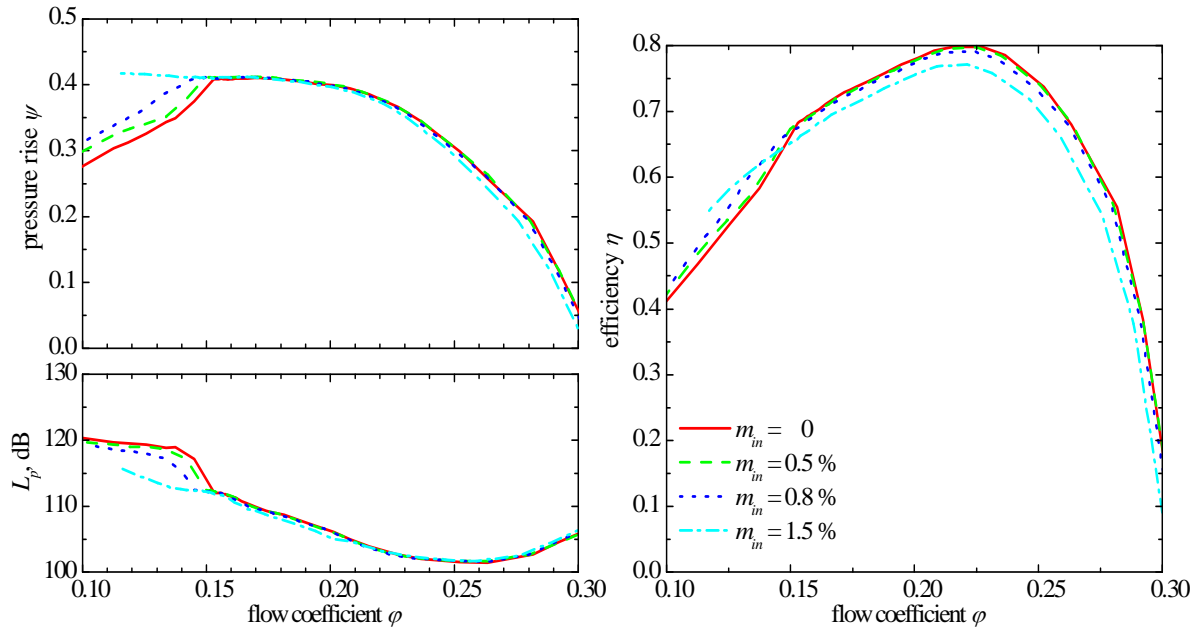


**Figure 13. Pressure coefficient, efficiency, and sound pressure in the outlet duct as functions of the flow coefficient for different steady air injection mass flows through the circumferential slit arrangement;  $n = 3000/\text{min}$ ,  $\zeta = 0.7\%$ ,  $\xi = 16.6\%$ .**

## VI. Conclusions

The secondary flow over the tip of the impeller blades of axial fans is important for the aerodynamic and acoustic performance of the fans. Pressure rise and efficiency drop, and the usable range of the performance characteristic is diminished as the rotor flow is stalled at higher flow rates. This is particularly so when the tip clearance gap is large. By applying active flow control in the tip regime of the impeller, it is possible to reduce the negative effects of the tip clearance flow. In the present paper, steady air injection into the tip clearance gap is investigated. An axial flow fan with  $D = 452.4$  mm impeller diameter is used for the experiments. The tip clearance gap is  $\zeta = s/c = 5.6\%$  of the blade chord at the tip. Four different air injection configurations are studied.

In the first configuration, air is injected through 24 slit nozzles placed uniformly over the circumference of the fan casing. With steady air injection it is possible to achieve either – with small injected mass flow rates – a significant reduction of the radiated noise level together with small improvements of the aerodynamic performance or – with high injected mass flow rates – significant improvements of the aerodynamic performance at the expense of a strong increase of the radiated noise level. The increase in noise level is caused by the interaction between the jets from the injection nozzles and the impeller blades, resulting in higher blade tone levels. The interaction of the 24 rotor blades with the 24 jets produces a blade passing frequency component propagating through the duct as a plane wave (see Tyler and Sofrin<sup>17</sup>) at all frequencies. The rotating instability component and the tip clearance noise are completely suppressed when the injected mass flow  $m_{in} \geq 0.6\%$ .

By appropriate choice of the number of injection nozzles, the unsteady forces generated by the rotor-jet-interaction can be made cut-off, i.e., the pressure fluctuations produced in the source region can not propagate as sound waves through the duct but decay exponentially with axial distance from the source. With 17 injection nozzles, the rotor-jet-interaction yields an azimuthal mode order  $m = 7$  for the blade passing frequency which is not propagational in the outlet duct. Consequently, the BPF-level in the outlet duct does not increase when the injected flow rate goes up. Similar to the air injection through 24 nozzles, significant improvements in the fan pressure are observed with steady air injection. In the case  $m_{in} = 1.5\%$ , the usable range of the fan characteristic is enlarged by 48%, and the fan pressure at the operating point  $\varphi = 0.149$  is increased from  $\psi = 0.29$  to 0.41. The fan efficiency is improved for small injection rates and low flow rates. At very high injection rates, the fan efficiency is impaired over a large regime of the flow coefficient because of the aerodynamic power necessary to produce the jet flow which is taken into account when calculating the efficiency.

Another method to avoid the increase in blade tone level is to replace the individual nozzles used before by a continuous circumferential slit in the fan casing. In this case, no unsteady forces are generated on the fan blades by the injected mass flow, and, hence, the blade passing frequency level is not altered. With this air injection configuration too, significant improvements of the aerodynamic and acoustic performance are achieved. With an injected mass flow of  $m_{in} = 1.5\%$ , the usable range of the fan characteristic is enlarged by 62%, and the fan pressure at the operating point  $\varphi = 0.137$  is increased from  $\psi = 0.29$  to 0.41. The efficiency is increased at low flow rates. The radiated sound pressure level is reduced over a large range of flow rates. The higher the injection rate, the larger the range of flow coefficient with reduced sound pressure level. For mass flow rates  $m_{in} \geq 0.8\%$ , rotating instability and tip clearance noise are suppressed.

In the fourth injection configuration studied, the air was blown into the tip clearance gap through the rotor blades and exiting from the blade tips. These experiments were made at a reduced fan speed because the air injection rates necessary for the design speed of  $n = 3000/\text{min}$  could not be delivered by the compressed air supply. With steady air injection, fan pressure and efficiency increase over the whole characteristic curve. The usable range of the fan characteristic is enlarged by 38%, and fan pressure and efficiency at the operating point  $\varphi = 0.175$  are increased from  $\psi = 0.32$  to 0.41 and  $\eta = 0.51$  to 0.62 with an injected mass flow rate of  $m_{in} = 0.3\%$ . The radiated sound pressure level is reduced with air injection. For mass flow rates  $m_{in} \geq 0.25\%$ , rotating instability and tip clearance noise are suppressed. The BPF-level increases with the injected mass flow but it is lower than with the other injection configurations.

Air injection into the tip clearance gap through the continuous circumferential slit in the fan casing was also tested with a small tip clearance gap of  $\zeta = 0.7\%$ . The usable range of the performance curve is enlarged also with the small tip clearance gap, however, this is the only positive effect found, which is in contrast to the results obtained with the large tip clearance gap where the air injection resulted in improvements of the aerodynamic and acoustic fan performance over wider ranges of the characteristic curve.

## Acknowledgments

The investigation is supported by the German National Science Foundation as part of the Sonderforschungsbereich 557 "Beeinflussung komplexer turbulenter Scherströmungen" conducted at the Technical University of Berlin.

## References

- <sup>1</sup>Kameier, F., "Experimentelle Untersuchungen zur Entstehung und Minderung des Blattspitzen-Wirbellärms axialer Strömungsmaschinen", VDI-Verlag, Düsseldorf, 1994, Diss., Fortschr.-Ber. VDI Reihe 7 Nr. 243.
- <sup>2</sup>Kameier, F., Neise, W., "Rotating blade flow instability as a source of noise in axial turbomachines", *Journal of Sound and Vibration*, Vol. 203, 1997, pp. 833-853.
- <sup>3</sup>Kameier, F., Neise, W., "Experimental study of tip clearance losses and noise in axial turbomachinery and their reduction", *ASME Journal of Turbomachinery*, Vol. 119, 1997, pp. 460 – 471.
- <sup>4</sup>März, J., Hah, Ch., Neise W., "An experimental and numerical investigation into the mechanisms of rotating instability", *ASME Journal of Turbomachinery*, 2002, Vol. 124, pp. 367 – 374.
- <sup>5</sup>Mailach, R., Lehmann, I., Vogeler, K., "Rotating instability in an axial compressor originating from the fluctuating blade tip vortex", *ASME Journal of Turbomachinery*, 2001, Vol. 123, pp. 453 – 460.
- <sup>6</sup>Legros, J.-C., Lemasson, M., Pauzin, S., "Contribution to noise reduction of an air conditioning turbomachine", *4<sup>th</sup> AIAA/CEAS Aeroacoustics Conference (19<sup>th</sup> AIAA Aeroacoustics Conference)*, AIAA-98-2254, Toulouse, France, 1998.
- <sup>7</sup>D'Andrea, R., Behnken, R. L., Murray, R. M., "Rotating stall control of an axial flow compressor using pulsed air injection." *ASME Journal of Turbomachinery*, 1997, Vol. 119, pp. 742 – 752.
- <sup>8</sup>Weigl, H. J., Paduano, J. D., Frechette, L. G., Epstein, A. H., Greitzer, E. M., Bright, M. M., Strazisar, A. J., "Active stabilization of rotating stall and surge in a transonic single-stage axial compressor", *ASME Journal of Turbomachinery*, 1998, Vol. 120, pp. 625 – 636.
- <sup>9</sup>Spakovszky, Z. S., Weigl, H. J., Paduano, J. D., van Schalkwyk, C. M., Suder, K. L., Bright, M. M., "Rotating stall control in a high-speed stage with inlet distortion: Part I – radial distortion", *ASME Journal of Turbomachinery*, 1999, Vol. 121, pp. 510 – 516.
- <sup>10</sup>Spakovszky, Z. S., van Schalkwyk, C. M., Weigl, H. J., Paduano, J. D., Suder, K. L., Bright, M. M., "Rotating stall control in a high-speed stage with inlet distortion: Part II – circumferential distortion", *ASME Journal of Turbomachinery*, 1999, Vol. 121, pp. 517 – 524.
- <sup>11</sup>Nie, C., Xu, G., Cheng, X., Chen, J., "Micro air injection and its unsteady response in a low-speed axial compressor", *ASME Journal of Turbomachinery*, 2002, Vol. 124, pp. 572 – 579.
- <sup>12</sup>Neuhaus, L., Neise, W., "Active control of the aerodynamic and acoustic performance of axial turbomachines", *8<sup>th</sup> AIAA/CEAS Aeroacoustics Conference*, AIAA-2002-2499, 17. – 19. June, Breckenridge, Colorado, USA, 2002.
- <sup>13</sup>Neuhaus, L., Neise, W., "Active control to improve the aerodynamic and acoustic performance of axial turbomachines", *1<sup>st</sup> Flow Control Conference*, AIAA-2002-2948, 24. – 27. June, St. Louis, Missouri, USA, 2002.
- <sup>14</sup>DIN 24163, *Ventilatoren, Teil 1 - 3 Leistungsmessung*. Deutsche Norm, Berlin, 1985, Deutsches Institut für Normung e.V.
- <sup>15</sup>ISO 5136, *Acoustics – Determination of sound power radiated into a duct by fans and other air-moving devices – In-duct method*, International Organization for Standardization Geneva, 2003.
- <sup>16</sup>Neuhaus, L., Neise, W., "Active flow control to reduce the tip clearance noise and improve the aerodynamic performance of axial turbomachines", *Fan Noise 2003*, 23.-25. September 2003, Senlis, France, 2003.
- <sup>17</sup>Tyler J. M., Sofrin T. G., "Axial Flow Compressor Noise Studies", *Transactions of the Society of Automotive Engineers*, 1962, Vol. 70, pp. 309-332.